Amino Acids (2013) 44:673–681
DOI 10.1007/s00726-012-1391-y

ORIGINAL ARTICLE

A novel radiofluorinated agouti-related protein for tumor angiogenesis imaging

Han Jiang · Sarah J. Moore · Shuanglong Liu · Hongguang Liu · Zheng Miao · Frank V. Cochran · Yang Liu · Mei Tian · Jennifer R. Cochran · Hong Zhang · Zhen Cheng

Received: 20 May 2012 / Accepted: 20 August 2012 / Published online: 4 September 2012

Abstract A novel protein scaffold based on the cystine knot domain of the agouti-related protein (AgRP) has been used to engineer mutants that can bind to the $\alpha_v\beta_3$ integrin receptor with high affinity and specificity. In the current study, an ^{18}F-labeled AgRP mutant (7C) was prepared and evaluated as a positron emission tomography (PET) probe for imaging tumor angiogenesis. AgRP-7C was synthesized by solid phase peptide synthesis and site-specifically conjugated with 4-nitrophenyl 2-$^{18/19}$F-fluoropropionate ($^{18/19}$F-NFP) to produce the fluorinated peptide, $^{18/19}$F-FP-AgRP-7C. Competition binding assays were used to measure the relative affinities of AgRP-7C and ^{19}F-FP-AgRP-7C to human glioblastoma U87MG cells that overexpress $\alpha_v\beta_3$ integrin. In addition, biodistribution, metabolic stability, and small animal PET imaging studies were conducted with ^{18}F-FP-AgRP-7C using U87MG tumor-bearing mice. Both AgRP-7C and ^{19}F-FP-AgRP-7C specifically competed with ^{125}I-echistatin for binding to U87MG cells with half maximal inhibitory concentration (IC_{50}) values of 9.40 and 8.37 nM, respectively. Non-invasive small animal PET imaging revealed that ^{18}F-FP-AgRP-7C exhibited rapid and good tumor uptake (3.24 percentage injected dose per gram [% ID/g] at 0.5 h post injection [p.i.]). The probe was rapidly cleared from the blood and from most organs, resulting in excellent tumor-to-normal tissue contrasts. Tumor uptake and rapid clearance were further confirmed with biodistribution studies. Furthermore, co-injection of ^{18}F-FP-AgRP-7C with a large molar excess of blocking peptide c(RGDyK) significantly inhibited tumor uptake in U87MG xenograft models, demonstrating the integrin-targeting specificity of the probe. Metabolite assays showed that the probe had high stability, making it suitable for in vivo applications. ^{18}F-FP-AgRP-7C exhibits promising in vivo properties such as rapid tumor targeting, good tumor uptake, and excellent tumor-to-normal tissue ratios, and warrants further investigation as a novel PET probe for imaging tumor angiogenesis.

Keywords Knottin · $\alpha_v\beta_3$ integrin · PET · ^{18}F

H. Jiang · Y. Liu · M. Tian · H. Zhang (✉)
Department of Nuclear Medicine, Second Affiliated Hospital of Zhejiang University School of Medicine, Institute of Nuclear Medicine and Molecular Imaging of Zhejiang University, Key Laboratory of Medical Molecular Imaging of Zhejiang Province, Hangzhou 310009, China
e-mail: hzhang21@gmail.com

H. Jiang · S. Liu · H. Liu · Z. Miao · Y. Liu · Z. Cheng (✉)
Department of Radiology, Molecular Imaging Program at Stanford (MIPS), Bio-X Program and Canary Center at Stanford for Cancer Early Detection, Stanford University, Stanford, CA 94305, USA
e-mail: zcheng@stanford.edu

S. J. Moore · F. V. Cochran · J. R. Cochran
Department of Bioengineering, Cancer Institute, Bio-X Program, Stanford University, Stanford, CA 94305, USA

Introduction

Small protein scaffolds are constrained polypeptides consisting of structural elements such as α-helix, β-sheet, and loop structures, with size ranges of 3–20 kDa (Miao et al. 2010). Rational and combinatorial methods have been used to engineer these scaffolds to bind to tumor-related receptors with low nanomolar or picomolar affinity. Tumor targets have included $\alpha_v\beta_3$ integrin, epidermal growth factor receptor, human epidermal growth factor receptor 2, tumor necrosis factor alpha, and carcinoembryonic antigen (Miao et al. 2010). Recently, engineered protein scaffolds have demonstrated much promise in the area of molecular

probe development. A myriad of protein scaffolds, including affibodies, cystine knot peptides, and ankyrin repeat proteins, have been engineered to bind to various tumor biomarkers and evaluated as in vivo molecular imaging agents (Cheng et al. 2008; Huang et al. 2008; Kimura et al. 2009a). These small protein scaffolds are highly structured and possess favorable properties such as rapid tumor accumulation, fast blood clearance, high in vivo stability, excellent biocompatibility, low immunogenicity and toxicity (Cheng et al. 2008, 2010; Miao et al. 2009; Ren et al. 2009).

Cystine knots (also known as knottins) are small, constrained polypeptides that share a common disulfide-bonded framework and triple-stranded β-sheet fold and possess one or more surface-exposed loops that bind diverse biological targets (Daly and Craik 2011; Kolmar 2010) The disulfide-bonded knottin core confers high stability in various chemical, physical, and biological environments. Furthermore, their relatively short amino acid sequences (typically 30–50 residues) allow them to be produced by chemical means such as solid-phase peptide synthesis. Several engineered knottins have been reported in the literature that bind to tumor-associated integrin receptors, including mutants derived from the *Ecballium elaterium* trypsin inhibitor II (EETI II) (Kimura et al. 2009a, b, 2010, 2011), α-amylase inhibitor tendamistat (Li et al. 2003), and agouti-related protein (AgRP) (Silverman et al. 2009).

The native AgRP is a neuropeptide produced in the human brain that plays an important role in the regulation of appetite and metabolism (Ollmann et al. 1997; Shutter et al. 1997; Backberg et al. 2004). A truncated form of AgRP (AgRP*), a 4-kDa cystine-knot peptide with four disulfide bonds and four solvent-exposed loops, has been successfully used as a scaffold for engineering peptides that bind to tumor angiogenesis biomarkers, such as $\alpha_v\beta_3$ integrins, with high affinity and specificity (Silverman et al. 2009). AgRP* has several distinct advantages as a scaffold for engineering tumor targeting agents (Kolmar 2010). The protein is of human origin, thus is expected to have low immunogenicity. In addition, its small size ($\sim$4 kDa) will impart fast blood clearance which is desirable for molecular imaging applications. The rigid AgRP* structure contains four solvent-accessible loops that could be mutated to engineer novel binding function. Finally, engineered AgRP-based knottins are amenable to recombinant or synthetic production, which allows site-specific incorporation of labels or chemical functionality for various applications.

In this study, for the first time, an AgRP knottin peptide (AgRP-7C) was site-specifically conjugated with a small ^{18}F prosthetic group, 4-nitrophenyl 2-^{18}F-fluoropropionate (^{18}F-NFP), through the peptide N-terminal amino group (Fig. 1). The resulting probe, ^{18}F-FP-AgRP-7C, was evaluated in nude mice bearing subcutaneous integrin-positive human glioblastoma U87MG xenografts.

Materials and methods

General

All 9-fluorenylmethyloxycarbonyl (Fmoc) protected amino acids were purchased from Novabiochem/EMD Chemicals Inc (La Jolla, CA) or CS Bio (Menlo Park, CA). ^{125}I-labeled echistatin was purchased from GE Healthcare Life Sciences (Piscataway, NJ). Phosphate buffered saline (PBS, 0.01 M, pH 7.4) was obtained from Gibco/Invitrogen (Carlsbad, CA). All other chemicals were purchased from Fisher Scientific (Fair Lawn, NJ) unless otherwise specified. The U87MG human glioblastoma cell line was obtained from American Type Culture Collection (Manassas, VA). Female athymic nude mice (nu/nu) were purchased from Charles River Laboratory (Wilmington, MA).

Semipreparative reversed-phase high performance liquid chromatography (RP-HPLC) using a Vydac protein and peptide column (218TP510; 5 μm, 250 × 10 mm) was performed on a Dionex 680 chromatography system with a UVD 170U absorbance detector and model 105S single-channel radiation detector (Carroll & Ramsey Associates, Berkley, CA). The recorded data were processed with use of Chromeleon version 6.50 software (Sunnyvale, CA). With a flow rate of 5.0 mL/min, the mobile phase was changed from 95 % solvent A (0.1 % trifluoroacetic acid [TFA] in water) and 5 % solvent B (0.1 % TFA in acetonitrile [MeCN]) to 35 % solvent A and 65 % solvent B over 32 min. Analytical HPLC had the same gradient system except that the flow rate was 1.0 mL/min with a Vydac protein and peptide column (218TP510; 5 μm, 250 × 4.6 mm). Absorbance was monitored at 218 nm, and peptide identification was based on the UV spectrum acquired using a PDA detector. All instruments, including matrix-assisted laser desorption/ionization time-of-flight mass spectrometry (MALDI-TOF–MS) instruments, RP-HPLC equipment including a radioaction detector, and a PET dose calibrator, were the same as those described previously (Cheng et al. 2007b).

Chemistry and radiochemistry

Linear AgRP-7C (sequence shown in Fig. 1) was synthesized with a CS BioCS336 instrument using Fmoc-based solid-phase peptide synthesis, and deprotected and cleaved from resin as reported previously (Jiang et al. 2010). Without intermediate purification, precursor peptide was oxidized and folded in 4 M guanidinium chloride, 10 mM

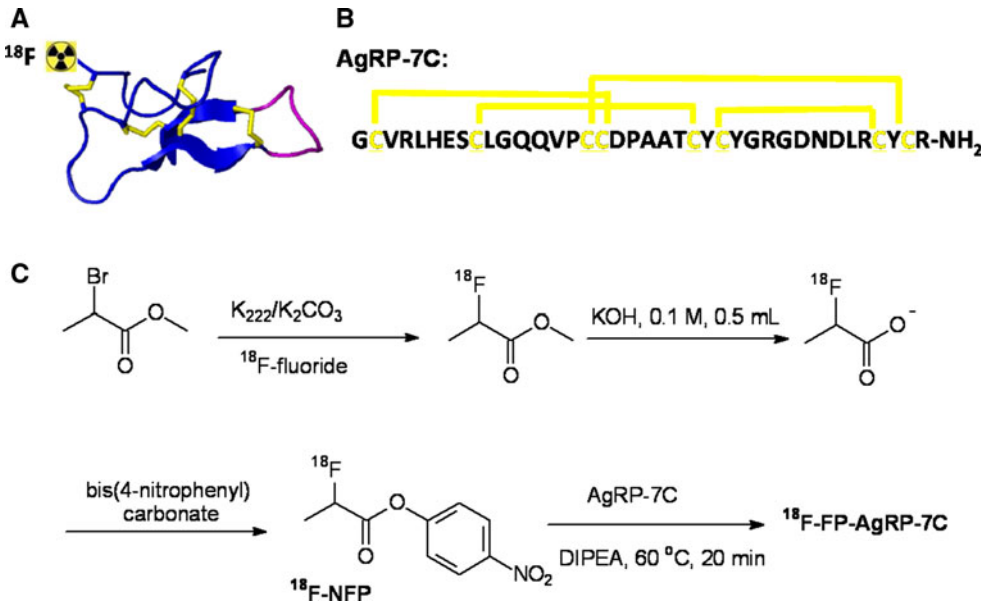

Fig. 1 Schematic and sequence of AgRP. **a** Structure of a radiofluorinated AgRP knottin scaffold. The imaging label 18F-NFP was site-specifically conjugated to the N terminus of the knottin peptide. **b** Amino acid sequence of AgRP-7C with disulfide bonds indicating the connectivity between Cys1-Cys4, Cys2-Cy5, Cys3-Cys8, and Cys6-Cys7. *Yellow lines* represent the disulfide bonds. **c** Synthetic scheme for 18F-NFP synthon and knottin radiofluorination

reduced glutathione, 2 mM oxidized glutathione, and 3.5 % (v/v) dimethylsulfoxide (DMSO) at pH 8.0 in ammonium bicarbonate buffer at room temperature for 3 days with gentle mixing. Folded peptide was purified on a Vydac C_{18} preparatory scale column to >95 % purity and lyophilized.

The synthesis of 4-nitrophenyl 2-fluoropropionate (^{19}F-NFP) is briefly described as follows: To a solution of 2-fluoropropionic acid (5.0 mg, 54.3 μmol) in 200 μL of dimethylformamide, bis(4-nitrophenyl) carbonate (15.2 mg, 50.0 μmol) and diisopropylethylamine (DIPEA; 20 μL) were added. After incubating at 60 °C for 3 h, the reaction mixture was cooled to room temperature and diluted with 1 mL of 5 % acetic acid solution. The product ^{19}F-NFP was isolated by semipreparative RP-HPLC. The collected fractions were combined, and the solvent was removed using a rotary evaporator. The product obtained was a white powder (5.9 mg, 56 %). ESI–MS: *m/z* 214.3 $[MH]^+$; ^{1}H NMR ($CDCl_3$, 300 MHz): $\delta = 8.24$ (d, $J = 9.0$ Hz, 2H), 7.27 (d, $J = 9.0$ Hz, 2H), 5.21 (m, 1H), 1.70 (dd, $J = 6.8$ Hz, 23.4 Hz, 3H). ^{13}C NMR ($CDCl_3$, 75 MHz): $\delta = 18.9$ (d, $J = 22.5$ Hz), 86.0 (d, $J =$ 184.0 Hz), 122.9, 126.0, 146.4, 155.2, 168.5. ^{19}F-NFP conjugated AgRP-7C (^{19}F-FP-AgRP-7C) was prepared as a reference compound. Briefly, AgRP-7C (0.5 mg, 0.12 μmol) was dissolved in 400 μL of dimethyl sulfoxide (DMSO) and ^{19}F-NFP (0.3 mg, 1.5 μmol) was dissolved in 100 μL of DMSO, and both solutions, along with 10 μL of DIPEA, were reacted for 1 h at room temperature. The resulting conjugate, ^{19}F-FP-AgRP-7C, was purified by the semipreparative RP-HPLC, and fractions containing the product were collected and lyophilized. The identity of ^{19}F-FP-AgRP-7C was confirmed by MALDI-TOF–MS.

^{18}F-NFP was prepared and used for AgRP-7C radiolabeling according to a previously reported protocol (Liu et al. 2010). ^{18}F-NFP (specific activity of 40–100 GBq/μmol, at the end of synthesis in 100 μL of DMSO) and 10 μL of DIPEA were added to 200 μg of AgRP-7C peptide and reacted for 20 min at 60 °C. After 1 mL of water containing 50 μL of TFA was added to quench the reaction, the radiolabeled product was separated by semipreparative HPLC using the same elution gradient as for ^{19}F-FP-AgRP-7C purification. The HPLC fractions containing ^{18}F-FP-AgRP-7C were collected and dried with a rotary evaporator. The radiolabeled peptide was reconstituted in PBS and passed through a 0.22–μm millipore (Billerica, MA) filter into a sterile vial for in vitro and in vivo experiments.

Cell culture and animal model

U87MG cells were cultured in Dulbecco's modified Eagle's high-glucose medium (GIBCO, Carlsbad, CA) and supplemented with 10 % fetal bovine serum (FBS) and 1 % penicillin–streptomycin in a humidified incubator containing 5 % CO_2 at 37 °C. A 70–80 % confluent monolayer was detached with 0.25 % trypsin–ethylenediaminetetraacetic acid (EDTA) and dissociated into a single-cell suspension for further cell culture and assays.

All animal studies were carried out in compliance with federal and local institutional rules for the conduct of animal experimentation. Approximately 5×10^6 cultured U87MG cells were suspended in 100 μL of PBS and subcutaneously implanted in the right shoulders of nude mice. Tumors were grown to a size of 0.5–1 cm in diameter (2–3 weeks).

U87MG cell uptake assay

Cell uptake studies were performed as previously described (Cheng et al. 2007a). Briefly, U87MG cells (3×10^5) were seeded in 12-well tissue culture plates and allowed to attach overnight. After a wash with 0.01 M PBS, the cells were incubated with ^{18}F-FP-AgRP-7C (37 kBq, 1 μCi per well, in culture medium) with or without c(RGDyK) (2 mg/well) at 37 °C for 1 and 2 h. The cells were then washed 3 times with PBS and lysed in 1 mL of 1.0 M NaOH and 0.1 % sodium dodecyl sulfate. Radioactivity was measured by using a γ-counter (PerkinElmer 1470, Waltham, MA). Cell uptake was expressed as the percentage of added radioactivity. Experiments were performed twice with triplicate wells.

U87MG cell binding assay

Cell binding assays were performed as previously described (Miao et al. 2009). Briefly, U87MG cells (2×10^5) were incubated with 0.06 nM ^{125}I-echistatin and varying concentrations of peptides (AgRP-7C and ^{19}F-FP-AgRP-7C) in integrin-binding buffer (25 mM Tris pH 7.4, 150 mM NaCl, 2 mM $CaCl_2$, 1 mM $MgCl_2$, 1 mM $MnCl_2$, and 0.1 % bovine serum albumin) at room temperature for 1 h. The cell-bound radioactivity remaining after washing was determined by γ-counting. The data were analyzed with use of GraphPad Prism (GraphPad Software, Inc. La Jolla, CA), and the concentration of unlabeled peptide required to inhibit 50 % of the ^{125}I-echistatin binding (IC_{50} value) was calculated. The experiment was performed with quadruplicate samples.

Small-animal PET imaging

Small-animal PET imaging was performed on a micro-PET R4 rodent model scanner (Concorde Microsystems Inc. Knoxville, TN). Mice bearing U87MG ($n = 4$ for each group) xenografts were injected via the tail vein with approximately 3.7 MBq (100 μCi) of ^{18}F-FP-AgRP-7C with or without 10 mg of c(RGDyK) per kg of mouse body weight. At 0.5, 1, and 2 h post-injection (p.i.), mice were anesthetized with 2 % isoflurane and placed in the prone position near the center of the field of view of the scanner. Five-minute static scans were obtained, and the images were reconstructed with use of a 2-dimensional ordered-subsets expectation maximization (OSEM) algorithm. No background correction was performed. Regions of interest (ROIs: 5 pixels for coronal and transaxial slices) were drawn over the tumor on decay-corrected whole-body coronal images. Maximum counts per pixel per minute were obtained from the ROIs and converted to counts per milliliter per minute by using a calibration constant. The percent injected radioactive dose per gram of tissue (% ID/g) values were determined by dividing counts per gram per minute by injected dose. No attenuation correction was performed.

Biodistribution studies

For biodistribution studies, nude mice bearing U87MG xenografts ($n = 4$ per group) were injected via the tail vein with approximately 3.7 MBq (100 μCi) of ^{18}F-FP-AgRP-7C with or without 10 mg of c(RGDyK) per kg of mouse body weight and euthanized at 2 h p.i. Tumor and normal tissues of interest were removed and weighed, and their radioactivity was measured in a γ-counter. Radioactivity uptake was expressed as the % ID/g.

In vivo metabolite analysis

The in vivo metabolic stability of ^{18}F-FP-AgRP-7C was determined from samples recovered from the tumor and several murine organs using a procedure described previously (Jiang et al. 2010). Briefly, ^{18}F-FP-AgRP-7C was injected into U87MG tumor-bearing mice via the tail vein, and the mice were euthanized at 1 h p.i. Urine was collected, and tumor, liver, and kidneys were homogenized and extracted with PBS and dimethylformamide (500 μL each). After centrifugation in Costar nylon filter tubes, samples were analyzed by reversed-phase HPLC using a radioactive detector (radio-HPLC), and compared to the untreated radiolabeled peptide.

Statistical methods

Statistical analysis was performed using the Student's t test for unpaired data. A 95 % confidence level was chosen to determine the significance between groups, with P values of less than 0.05 being designated as significantly different.

Results

Chemistry and radiochemistry

AgRP-7C was synthesized by solid phase peptide synthesis, folded in vitro, and purified by RP-HPLC. ^{19}F-FP-AgRP-7C was prepared by site-specific conjugation of ^{19}F-NFP to the N terminus of AgRP-7C with a 92 % yield. This non-radioactive analog was used as a standard for radiosynthesis and integrin receptor binding assays. The product purities were more than 95 %, as determined by analytical HPLC, and the molecular masses were characterized by MALDI-TOF–MS. Folded peptide AgRP-7C: $m/z = 4222.5$ for $[MH]^+$ ($C_{171}H_{259}N_{55}O_{55}S_8$, calculated

$[MH]^+ = 4221.8$ after accounting for the loss of 8 protons upon formation of 4 disulfide bonds). ^{19}F-FP-AgRP-7C: $m/z = 4297.3$ for $[MH]^+$ ($C_{174}H_{262}FN_{55}O_{56}S_8$, calculated $[MH]^+ = 4295.8$). The retention times on analytical HPLC for folded AgRP-7C and ^{19}F-FP-AgRP-7C were 14.3 and 18.3 min, respectively.

For radiolabeling, the synthesis time for ^{18}F-NFP was approximately 100 min, and the decay corrected yield was 67 ± 11 % using a modified GE synthetic module (TRACERlab FXFN) (Liu et al. 2010; Haubner et al. 2001). Counted from ^{18}F-NFP, the radiochemical yield of ^{18}F-FP-AgRP-7C (decay corrected) was generally greater than 70 %. Because the unlabeled AgRP-7C could be easily separated from the ^{18}F-FP-AgRP-7C, the radiochemical purity of ^{18}F-FP-AgRP-7C was >95 % according to analytic HPLC, and the specific radioactivity of the probe was estimated to be 20–40 GBq/μmol on the basis of the prosthetic labeling agent ^{18}F-NFP.

In vitro cell uptake

U87MG cell uptake of ^{18}F-FP-AgRP-7C was performed to evaluate integrin binding and specificity. Levels of cell uptake of ^{18}F-FP-AgRP-7C were observed after 1 h and 2 h incubation at 37 °C (Fig. 2a). ^{18}F-FP-AgRP-7C exhibited high accumulation in U87MG cells, with uptake values reaching about 3 % of applied activity at 1 h. Furthermore, probe accumulation was efficiently inhibited by the addition of unlabeled c(RGDyK) ($P < 0.05$), an integrin-binding peptidomimetic, indicating that ^{18}F-FP-AgRP-7C specifically targets integrin receptors.

The relative receptor binding affinities of AgRP-7C and ^{19}F-FP-AgRP-7C were determined by competitive binding assays with ^{125}I-echistatin. Both peptides inhibited the binding of ^{125}I-echistatin to U87MG cells in a concentration-dependent manner (Fig. 2b), with IC_{50} values of 9.4 ± 1.8 and 8.4 ± 2.3 nM for AgRP-7C and ^{19}F-FP-AgRP-7C, respectively. Therefore, the N-terminal fluoropropionate modification had no effect on the integrin-binding affinity of AgRP-7C.

Small-animal PET imaging

Decay-corrected coronal PET images of a U87MG tumor-bearing mouse at 0.5, 1, and 2 h p.i., of ^{18}F-FP-AgRP-7C were obtained by micro PET imaging (Fig. 3a). The tumor was clearly visible at 0.5 h p.i., and enhanced tumor-to-background contrast was achieved at 2 h. The probe showed rapid clearance from blood and most normal organs, and low accumulation in lung, liver, and abdominal regions were observed, resulting in excellent tumor imaging quality. Relatively high levels of radioactivity accumulation and retention were observed in the kidneys.

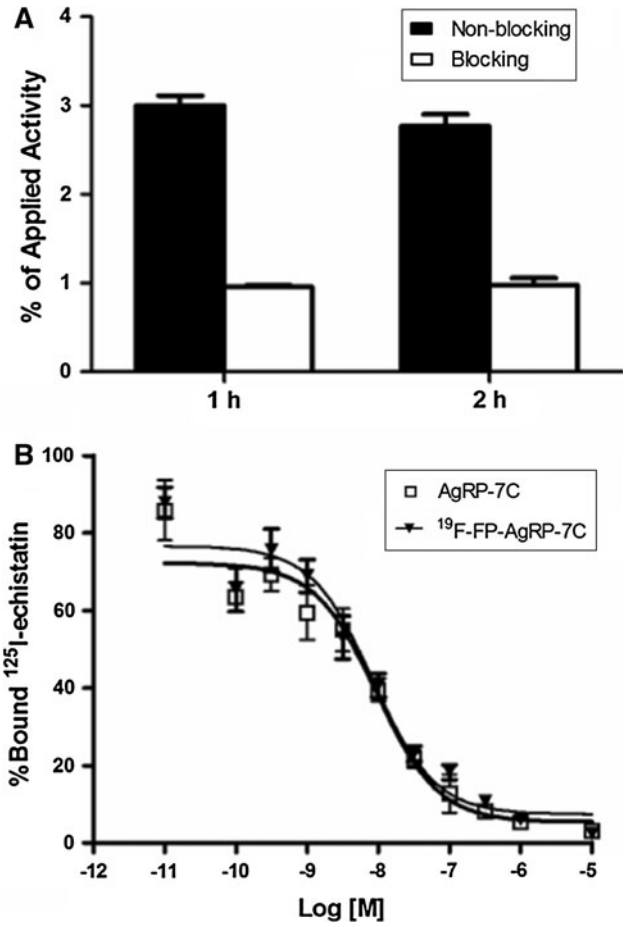

Fig. 2 **a** In vitro U87MG cell uptake assay. U87MG cells were incubated with 37 kBq (1 μCi) of ^{18}F-FP-AgRP-7C for 1 and 2 h at 37 °C, with or without c(RGDyK) as a blocking agent. Data represent the mean percentage of total radioactivity added. The experiment was performed in triplicate, and the error bars represent standard deviation. **b** Competition binding of ^{125}I-echistatin binding to integrin receptors on U87MG cells by AgRP-7C and ^{19}F-FP-AgRP-7C (IC_{50} = 9.4 ± 1.8 and 8.4 ± 2.3 nM, respectively). Results are expressed as the mean of quadruplicate measurements ± standard deviation

Co-injection of excess c(RGDyK) as a blocking agent significantly reduced tumor uptake, which confirmed the in vivo tumor-targeting specificity of the probe. In addition, no visible bone uptake was observed in any PET images, suggesting no defluorination of the probe. Tumor and major organ activity accumulation was quantified by measuring the ROIs encompassing the entire organ on the coronal images (Fig. 3b). ^{18}F-FP-AgRP-7C displayed good tumor uptake and retention, with values of 3.24 ± 0.33, 2.39 ± 0.15, and 1.51 ± 0.19 % ID/g observed at 0.5, 1, and 2 h, respectively. For the blocking group, the tumor uptake value was only 0.97 ± 0.27 % ID/g at 1 h p.i. ($P < 0.05$), indicating 59.4 % inhibition. ^{18}F-FP-AgRP-7C was also rapidly cleared from the blood, with the highest uptake value of 1.16 ± 0.11 % ID/g observed at 0.5 h.

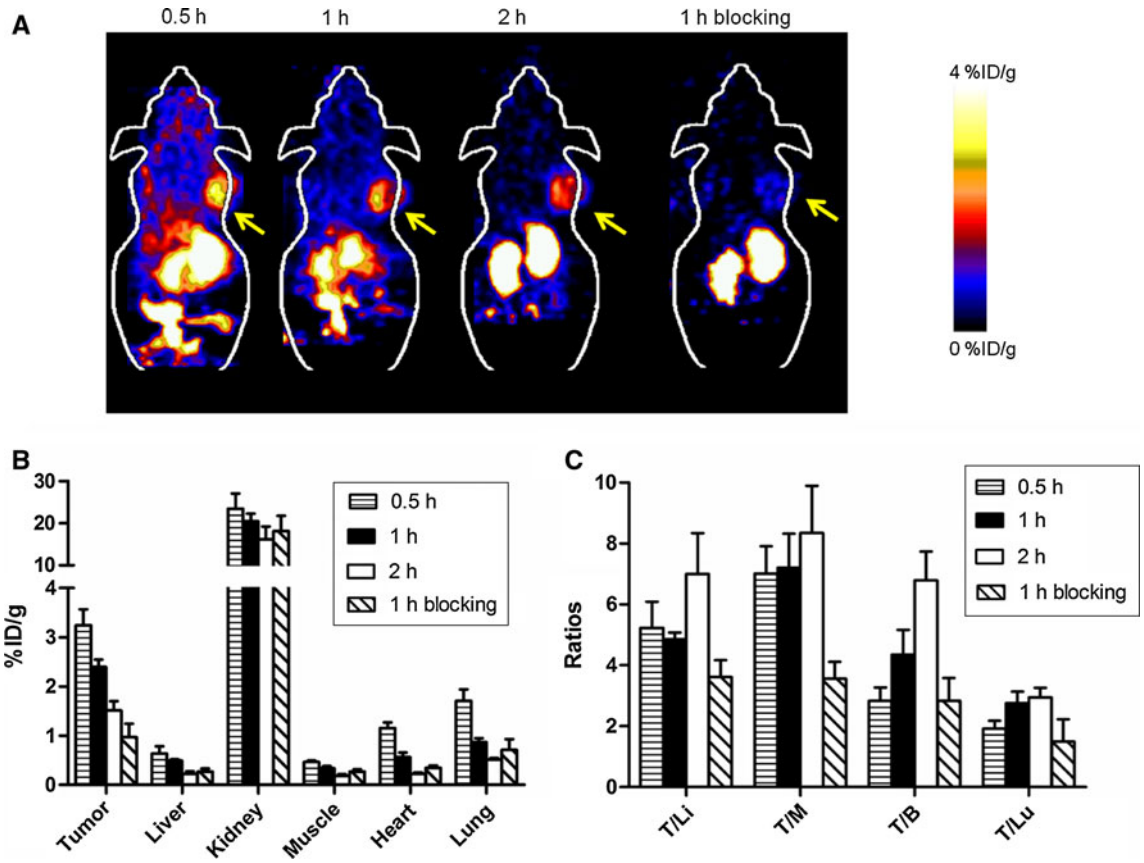

Fig. 3 PET imaging of ^{18}F-FP-AgRP-7C in nude mice bearing U87MG tumor xenografts ($n = 4$ per group). **a** Coronal PET images of U87MG tumor-bearing mice at 0.5, 1, and 2 h post injection of approximately 3.7 MBq (100 μCi) of ^{18}F-FP-AgRP-7C with or without 10 mg c(RGDyK) per kg of mouse body weight at 1 h after injection. *Arrows* indicate the location of tumors. **b** Small animal PET quantification results, expressed as % ID/g, in various organs and tumors after injection of ^{18}F-FP-AgRP-7C. **c** Tumor-to-normal tissue ratios at 0.5, 1, and 2 h p.i. (T/Li, T/M, T/B and T/Lu represent tumor-to-liver, tumor-to-muscle, tumor-to-blood and tumor-to-lung ratios, respectively)

Muscle uptake was also very low (<0.5 % ID/g) at all times tested. The tumor-to-muscle, tumor-to-blood, and tumor-to-liver ratios were 7.0, 2.8 and 5.2, respectively, at 0.5 h (Fig. 3c).

Biodistribution studies

Biodistribution studies confirmed that the probe had good uptake in tumors and low accumulation in most normal organs (Fig. 4). Tumor uptake of ^{18}F-FP-AgRP-7C was 1.49 ± 0.20 % ID/g at 2 h p.i., whereas for most of normal organs, the uptake of the probe was lower than 1 % ID/g. Furthermore, for the blocking group, tumor uptake (0.57 ± 0.14 % ID/g at 2 h p.i.) was significantly lower than that of the control group ($P < 0.05$), demonstrating integrin receptor-mediated tumor targeting of the probe. Finally, the corresponding organ uptakes obtained from biodistribution were consistent with the PET quantification results, and no significant differences were observed between these two studies.

In vivo metabolite analysis

^{18}F-FP-AgRP-7C showed high stability in PBS with no free ^{18}F or other catabolic products as assayed by radio-HPLC (Fig. 5a). In vivo metabolite analyses were also conducted in tumor, liver, kidney, and urine samples, which were obtained from the U87MG tumor-bearing mice at 1 h after injection of the probe (Fig. 5b–e). Only minor peaks with retention times between 5 and 10 min were observed in tested samples. These results suggest that ^{18}F-FP-AgRP-7C is highly metabolically stable in vivo.

Discussion

Knottins have generated substantial interest in recent years in the development of molecular imaging probes because of their high stability, facile synthesis, and potential for site-specific labeling. In the current study, we first demonstrated that AgRP-7C can be site-specifically

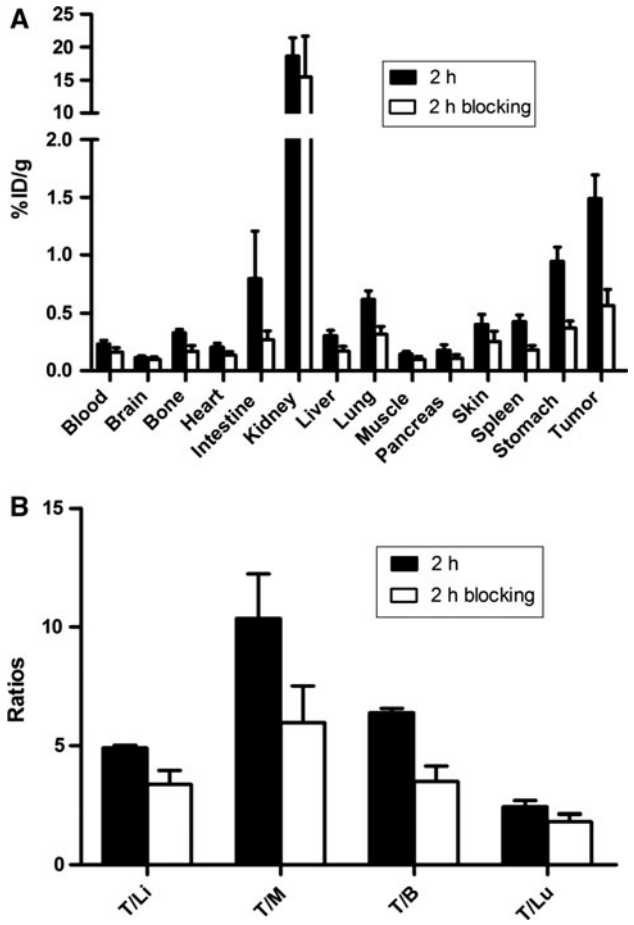

Fig. 4 Biodistribution and tumor-to-normal tissue ratios of ^{18}F-FP-AgRP-7C in U87MG tumor-bearing nude mice 2 h after injection of approximately 3.7 MBq (100 μCi) of ^{18}F-FP-AgRP-7C with or without co-injection of 10 mg c(RGDyK) per kg mouse body weight. Data are expressed as % ID/g ± SD ($n = 4$ per group). *T/Li*, *T/M*, *T/B* and *T/Lu* represent tumor-to-liver, tumor-to-muscle, tumor-to-blood and tumor-to-lung ratios, respectively

radiofluorinated and used for in vivo imaging of integrin-positive tumors. The whole study highlights the high potential of AgRP knottins for probe development.

^{18}F-NFP was selected as a prosthetic group for site-specific labeling of AgRP-7C because of its small size, high in vivo stability, and well-established production method in our program (Liu et al. 2010). The nonradioactive probe, ^{19}F-FP-AgRP-7C, was prepared as a reference compound and possessed similar relative binding affinity compared to that of the unlabeled peptide, indicating that AgRP-7C can preserve its bioactivity when modified with a small tag such as NFP. These modifications didn't influence the binding affinity with $\alpha_v\beta_3$ integrin, which was confirmed by the binding assay, raveling the high affinity and selective binding. Cell uptake studies performed in the presence and absence of blocking peptide also demonstrated that the probe can specifically bind to integrin receptors. The metabolic stability of ^{18}F-FP-AgRP-7C was performed in tumor, liver, kidney and urine. The result displayed high in vivo stability, more stable than ^{18}F-Galacto-RGD (Haubner et al. 2004).

Compared with large protein scaffold, AgRP* has small molecular weight. Small size allows it to clear through the kidney rather than the liver, allowing for visualization of tumors located in the abdominal area in molecular imaging applications. It enables fast targeting to the tumor and quick clearance from the other organs. In a previous study, we used a conventional radiofluorination synthon, *N*-succinimidyl-4-^{18}F-fluorobenzoate (^{18}F-SFB) to radiofluorinate an EETI-II based knottin peptide (2.5D) that binds with integrins with low nanomolar affinity. PET imaging showed that ^{18}F-SFB-labeled 2.5D (^{18}F-FB-2.5D) had a relatively fast tumor washout rate and high uptake in gallbladder and liver, indicating the suboptimal pharmacokinetics of the probe and low in vivo stability of ^{18}F-FB-2.5D, which limits the further clinical application for tumor imaging (Miao et al. 2009). In the current study, ^{18}F-FP-AgRP-7C showed much better tumor-imaging quality because of higher tumor uptake (for example, 3.24 ± 0.33 vs. ~2 ± 0.72 % ID/g at 0.5 h p.i.), better tumor retention, and lower uptake in many normal organs. Furthermore, the in vivo receptor targeting specificity of the probe was demonstrated by blocking experiments, in which unlabeled c(RGDyK) peptide significantly inhibited tumor uptake. Of note, kidney uptake of ^{18}F-FP-AgRP-7C was 18.9 ± 2.75 % ID/g at 2 h p.i., which was much lower than that of ^{64}Cu-DOTA-AgRP-7C (60.22 ± 17.52 % ID/g) (Jiang et al. 2010), suggesting an advantage to using ^{18}F as a PET label. Moreover, compared with ^{64}Cu-DOTA-AgRP-7C, ^{18}F-FP-AgRP-7C also displayed reduced accumulation in liver (0.31 ± 0.05 vs. 1.74 ± 0.72 % ID/g). In contrast to the high-activity concentration found in the kidneys due to the renal elimination, no increase activity in the gut was showed, indicating that there is no significant biliary excretion of the tracer into the intestine during the observation period of 2 h. Low radioactivity accumulation in liver of ^{18}F-FP-AgRP-7C results in its potential clinical application for tumor detection in liver. The background activity in muscle tissue and blood pool was very low. The absence of radioactivity accumulation in the skeletal system in PET images revealed no defluorination of ^{18}F-FP-AgRP-7C. The background radioactivity of other organs was low and decreased with time, creating good contrasts. In vivo evaluation revealed that the probe exhibits fast tumor targeting and high tumor retention, rapid clearance from most normal tissues, and excellent tumor discrimination. These properties indicate promise for further development of ^{18}F-labeled peptides based on the AgRP* scaffold for tumor imaging applications.

Recently, cancer treatment targeting integrin $\alpha_v\beta_3$, such as MEDI-522 (a humanized anti-human integrin $\alpha_v\beta_3$

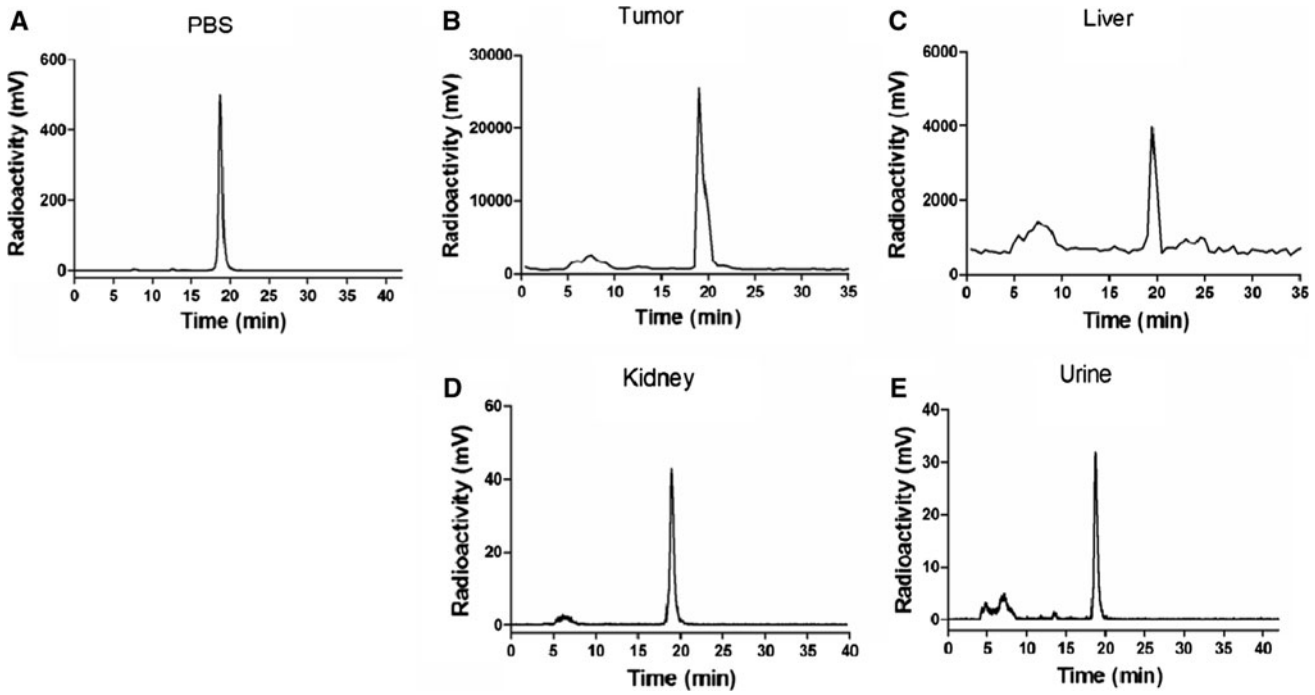

Fig. 5 In vivo metabolite assay. **a** ^{18}F-FP-AgRP-7C after incubation with PBS for 1 h. **b–e** Urine or homogenized tissues obtained from mice 1 h post injection of ^{18}F-FP-AgRP-7C. Probe stability was analyzed by radio-HPLC and γ-counting

monoclonal antibody) (Hersey et al. 2010) are in clinical trials for antiangiogenic therapy. Numerous patents have been administrated with $\alpha_v\beta_3$ antagonists for the prevention and/or treatment of cancer in the past several years. Meanwhile, clinical trials for evaluating the antagonists antiangiogenic and anti-tumor results in patients have been initiated, especially using PET imaging as a powerful tool to examine the effect of antiangiogenic therapies directly. A range of radionuclides (e.g., ^{18}F, ^{64}Cu, and ^{99m}Tc) can be carried into the RGD peptides as a targeting biomarker to the $\alpha_v\beta_3$ integrin in various malignant tumors (Beer et al. 2008; Haubner et al. 2003). Radiolabeled RGD peptide used for detection of $\alpha_v\beta_3$ integrin-receptor positive tumors before and/or after the administration of the antagonists, permits the selection of the patients and optimization of the treatments strategies. As demonstrated in this study, ^{18}F-FP-AgRP-7C will be a potential candidate for predicting and evaluating the antiangiogenic treatment by PET imaging. Furthermore, AgRP-7C can be radiolabeled with different therapeutic isotopes to generate a series of agents for integrin-targeted internal radiotherapy. Additionally, the important issue in clinical application might be that the use of ^{18}F-FP-AgRP-7C in human is not expected to have immunogenicity and toxicity because of its human origin and low plasma concentration.

The current study has some limitations. A major drawback was high renal uptake. The probe needs further modification to reduce the kidney accumulation. Administration of a diuretic agent (e.g., furosemide) together with the tracer similar to protocols used for imaging with ^{18}F-FDG also can reduce the activity concentration in the kidney. Although the data in brain was encouraging, future studies on brain primary and metastatic tumor models require to be done for further demonstrating the hypothesis that ^{18}F-FP-AgRP-7C could cross BBB. Moreover, it will require tracer kinetic analysis, traditional Western blots, in vitro receptor autoradiography and immunohistochemistry to detect the relationship between in vivo imaging and expression $\alpha_v\beta_3$ integrin of tumors. The in vivo data was obtained from mice models and can't accurately mimic the complex human situation. Thus, we need better animal models to demonstrate the potential clinical application of ^{18}F-FP-AgRP-7C.

Conclusion

In this study, ^{18}F-FP-AgRP-7C shows high $\alpha_v\beta_3$ integrin-binding affinity and specificity in vitro. Biodistribution and small animal PET imaging studies further demonstrated that ^{18}F-FP-AgRP-7C is a promising PET probe for imaging $\alpha_v\beta_3$ integrin-positive tumors in living subjects. ^{18}F-FP-AgRP-7C exhibits desirable in vivo properties such as rapid tumor targeting, high tumor uptake and retention, and good tumor-to-normal tissue ratios. The promising properties of ^{18}F-FP-AgRP-7C reveal that this probe can be a powerful tool to evaluate the $\alpha_v\beta_3$ integrin overexpression tumors in basic researches as well as clinical application. In

addition, this work further validates the potential of AgRP*-based peptides for molecular imaging applications.

Acknowledgments This work was supported, in part, by National Cancer Institute (NCI) 5R01 CA119053, NCI In Vivo Cellular Molecular Imaging Center (ICMIC) grant P50 CA114747, NCI 5K01 CA104706, and a Stanford Molecular Imaging Scholars postdoctoral fellowship R25 CA118681. SJM has been supported by an NSF Graduate Research Fellowship, the Medtronic Stanford Graduate Fellowship, and a Siebel Scholars Fellowship. This work is also partly sponsored by Grants from the Zhejiang Provincial Natural Science Foundation of China (Z2110230), Health Bureau of Zhejiang Province (2010ZA075, 2011ZDA013), National Science Foundation of China (NSFC) (no. 81101023, 81170306, 81173468), and Ministry of Science and Technology of China (2012BAI13B06). The authors acknowledge Tamara Locke for help on editing the manuscript.

Conflict of interest The authors declare that they have no conflict of interest.

References

Backberg M, Madjid N, Ogren SO, Meister B (2004) Down-regulated expression of agouti-related protein (AGRP) mRNA in the hypothalamic arcuate nucleus of hyperphagic and obese tub/tub mice. Brain Res Mol Brain Res 125(1–2):129–139. doi:10.1016/j.molbrainres.2004.03.012

Beer AJ, Niemeyer M, Carlsen J, Sarbia M, Nahrig J, Watzlowik P, Wester HJ, Harbeck N, Schwaiger M (2008) Patterns of alphavbeta3 expression in primary and metastatic human breast cancer as shown by 18F-Galacto-RGD PET. J Nucl Med 49(2):255–259. doi:10.2967/jnumed.107.045526

Cheng Z, Xiong Z, Subbarayan M, Chen X, Gambhir SS (2007a) 64Cu-labeled alpha-melanocyte-stimulating hormone analog for microPET imaging of melanocortin 1 receptor expression. Bioconjug Chem 18(3):765–772. doi:10.1021/bc060306g

Cheng Z, Zhang L, Graves E, Xiong ZM, Dandekar M, Chen XY, Gambhir SS (2007b) Small-animal PET of melanocortin 1 receptor expression using a F-18-labeled alpha-melanocyte-stimulating hormone analog. J Nucl Med 48(6):987–994. doi:10.2967/jnumed.107.039602

Cheng Z, De Jesus OP, Namavari M, De A, Levi J, Webster JM, Zhang R, Lee B, Syud FA, Gambhir SS (2008) Small-animal PET imaging of human epidermal growth factor receptor type 2 expression with site-specific 18F-labeled protein scaffold molecules. J Nucl Med 49(5):804–813. doi:10.2967/jnumed.107.047381

Cheng Z, De Jesus OP, Kramer DJ, De A, Webster JM, Gheysens O, Levi J, Namavari M, Wang S, Park JM, Zhang R, Liu H, Lee B, Syud FA, Gambhir SS (2010) 64Cu-labeled affibody molecules for imaging of HER2 expressing tumors. Mol Imaging Biol 12(3):316–324. doi:10.1007/s11307-009-0256-6

Daly NL, Craik DJ (2011) Bioactive cystine knot proteins. Curr Opin Chem Biol. doi:10.1016/j.cbpa.2011.02.008

Haubner R, Wester HJ, Weber WA, Mang C, Ziegler SI, Goodman SL, Senekowitsch-Schmidtke R, Kessler H, Schwaiger M (2001) Noninvasive imaging of alpha(v)beta3 integrin expression using 18F-labeled RGD-containing glycopeptide and positron emission tomography. Cancer Res 61(5):1781–1785

Haubner RH, Wester HJ, Weber WA, Schwaiger M (2003) Radiotracer-based strategies to image angiogenesis. Q J Nucl Med 47(3):189–199

Haubner R, Kuhnast B, Mang C, Weber WA, Kessler H, Wester HJ, Schwaiger M (2004) [18F]Galacto-RGD: synthesis, radiolabeling, metabolic stability, and radiation dose estimates. Bioconjug Chem 15(1):61–69. doi:10.1021/bc034170n

Hersey P, Sosman J, O'Day S, Richards J, Bedikian A, Gonzalez R, Sharfman W, Weber R, Logan T, Buzoianu M, Hammershaimb L, Kirkwood JM (2010) A randomized phase 2 study of etaracizumab, a monoclonal antibody against integrin alpha(v)-beta(3), + or − dacarbazine in patients with stage IV metastatic melanoma. Cancer 116(6):1526–1534. doi:10.1002/cncr.24821

Huang L, Gainkam LO, Caveliers V, Vanhove C, Keyaerts M, De Baetselier P, Bossuyt A, Revets H, Lahoutte T (2008) SPECT imaging with 99mTc-labeled EGFR-specific nanobody for in vivo monitoring of EGFR expression. Mol Imaging Biol 10(3):167–175. doi:10.1007/s11307-008-0133-8

Jiang L, Kimura RH, Miao Z, Silverman AP, Ren G, Liu H, Li P, Gambhir SS, Cochran JR, Cheng Z (2010) Evaluation of a (64)Cu-labeled cystine-knot peptide based on agouti-related protein for PET of tumors expressing alphavbeta3 integrin. J Nucl Med 51(2):251–258. doi:10.2967/jnumed.109.069831

Kimura RH, Cheng Z, Gambhir SS, Cochran JR (2009a) Engineered knottin peptides: a new class of agents for imaging integrin expression in living subjects. Cancer Res 69(6):2435–2442. doi:10.1158/0008-5472.CAN-08-2495

Kimura RH, Levin AM, Cochran FV, Cochran JR (2009b) Engineered cystine knot peptides that bind alphavbeta3, alphavbeta5, and alpha5beta1 integrins with low-nanomolar affinity. Proteins 77(2):359–369. doi:10.1002/Prot.22441

Kimura RH, Miao Z, Cheng Z, Gambhir SS, Cochran JR (2010) A dual-labeled knottin peptide for PET and near-infrared fluorescence imaging of integrin expression in living subjects. Bioconjugate Chem 21(3):436–444. doi:10.1021/Bc9003102

Kimura RH, Jones DS, Jiang L, Miao Z, Cheng Z, Cochran JR (2011) Functional mutation of multiple solvent-exposed loops in the Ecballium elaterium trypsin inhibitor-II cystine knot miniprotein. PLoS One 6(2):e16112. doi:10.1371/journal.pone.0016112

Kolmar H (2010) Engineered cystine-knot miniproteins for diagnostic applications. Expert Rev Mol Diagn 10(3):361–368. doi:10.1586/erm.10.15

Li RH, Hoess RH, Bennett JS, DeGrado WF (2003) Use of phage display to probe the evolution of binding specificity and affinity in integrins. Protein Eng 16(1):65–72. doi:10.1093/proeng/gzg002

Liu S, Liu Z, Chen K, Yan Y, Watzlowik P, Wester HJ, Chin FT, Chen X (2010) 18F-labeled galacto and PEGylated RGD dimers for PET imaging of alphavbeta3 integrin expression. Mol Imaging Biol 12(5):530–538. doi:10.1007/s11307-009-0284-2

Miao Z, Ren G, Liu H, Kimura RH, Jiang L, Cochran JR, Gambhir SS, Cheng Z (2009) An engineered knottin peptide labeled with 18F for PET imaging of integrin expression. Bioconjug Chem 20(12):2342–2347. doi:10.1021/bc900361g

Miao Z, Levi J, Cheng Z (2010) Protein scaffold-based molecular probes for cancer molecular imaging. Amino Acids. doi:10.1007/s00726-010-0503-9

Ollmann MM, Wilson BD, Yang YK, Kerns JA, Chen Y, Gantz I, Barsh GS (1997) Antagonism of central melanocortin receptors in vitro and in vivo by agouti-related protein. Science 278(5335):135–138

Ren G, Zhang R, Liu Z, Webster JM, Miao Z, Gambhir SS, Syud FA, Cheng Z (2009) A 2-helix small protein labeled with 68 Ga for PET imaging of HER2 expression. J Nucl Med 50(9):1492–1499. doi:10.2967/jnumed.109.064287

Shutter JR, Graham M, Kinsey AC, Scully S, Luthy R, Stark KL (1997) Hypothalamic expression of ART, a novel gene related to agouti, is up-regulated in obese and diabetic mutant mice. Gene Dev 11(5):593–602

Silverman AP, Levin AM, Lahti JL, Cochran JR (2009) Engineered cystine-knot peptides that bind alpha(v)beta(3) integrin with antibody-like affinities. J Mol Biol 385(4):1064–1075. doi:10.1016/j.jmb.2008.11.004